Milstein Schemes in Monte Carlo

Kamlesh Sahoo (12821721), Yuhao Qian (13011456), Zhiyu Zhang (12986348)

I. Introduction

MILSTEIN scheme is a discretization technique to approximate the numerical solution of a stochastic differential equation (SDE). It is named after Grigori N. Milstein who first made the publication in 1974[8]. In contrast to the more conventional Euler-Maruyama (EM) discretization scheme, Milstein improves accuracy by expanding the coefficients of the drift and diffusion terms of the SDE and applying Ito's Lemma.

When it comes to pricing an option in real operation, it is essential to employ models and simulations that are accurate enough while don't require overly frequent evaluation. Here the two most well known option pricing models were considered: the Black-Scholes model with fixed volatility and the Heston model which takes into account stochastic volatility. Both the EM and Milstein schemes were explored using Monte-Carlo simulations with respect to the path-independent European options and path-dependent Barrier options.

In the case of the Black-Scholes model, exact solutions exist for both option types which can be used as benchmarks to compare the performance of the discretization schemes. However, for the Heston model, closed-form solutions are only semi-exact[5][3] and an alternative - *Almost Exact Solution (AES)*[9] was used instead.

In this paper, we first present the theoretical background of option pricing models and discretization schemes, along with the theory of error and convergence. We then perform numerical simulations of stock price paths and price the options based on these simulated paths. Finally, we analyze and explore the errors in both discretization schemes.

II. Option Pricing Models

A. European option

An option is a contract that enables but does not obligate its holder to buy or sell the underlying asset at a predetermined strike price of K by a specific expiration date[6]. The European option is the simplest type of option. The holder of the European option can only exercise at maturity, which means the value of the option only depends on the underlying asset price at the expiration date. For a European call option the payoff function is given by:

$$f(S_T) = \max\{S_T - K, 0\} \tag{1}$$

while the payoff function for put option is:

$$f(S_T) = \max\{K - S_T, 0\} \tag{2}$$

where S_T is the stock price at maturity and K the strike price.

B. Barrier option

Barrier option is one of the classic path-dependent options. The unique feature is that the payoff of the barrier option is not only dependent on the underlying asset's final price but also on whether or not the asset price reached a certain level during the life of the option[1].

The barrier option can be classified as either a knock-out option or a knock-in option. A knock-out option is one where the option is invalid if the underlying asset price reaches a specific barrier before maturity; a knock-in option is another type of barrier option which comes into existence only when the underlying asset price touches a barrier. Based on the direction of stock price movement, knock-out options are further classified as down-and-out and up-and-out options. Similarly, knock-in options can be classified as down-and-in and up-and-in options. We only concentrate on the down-and-out option in this assignment.

For a down-and-out call option, payoff is:

$$V_{DO} = (S_T - K)^+ \mathbf{1}_{(S_t > H)} \tag{3}$$

where $\mathbf{1}_{(S_t>H)}$ is an indicator function. The indicator function equals to one if the underlying asset price is always above the barrier H, $H < S_0$ during the life of the option.

C. Black Scholes

The Black-Scholes model is utilized to evaluate stocks and other financial assets. The model assumes a Geometric Brownian motion to be the underlying factor of the stock. This Geometric Brownian motion is described by the equation below:

$$dS_t = rS_t dt + \sigma S_t dW_t \tag{4}$$

where:

- r : continuously compounded annual interest rate
- σ : volatility ($\sigma \geq 0$)
- dW_t : a Wiener processe($dW_t \sim \mathcal{N}(0, dt)$)

1) Analytical value of European option in Black Scholes: Black Scholes Merton differential equation is derive from equation 4:

$$\frac{\partial f}{\partial t} + rS\frac{\partial f}{\partial S} + \frac{1}{2}\sigma^2 S^2 \frac{\partial^2 f}{\partial S^2} = rf \tag{5}$$

This equation's solution gives the prices of European call and put options:

$$C = S_0 N(d_1) - Ke^{-rT} N(d_2) \tag{6}$$

$$P = Ke^{-rT} N\left(-d_2\right) - S_0 N\left(-d_1\right) \tag{7}$$

where:

$$d_1 = \frac{\log\left(S_0/K\right) + \left(r + \sigma^2/2\right) T}{\sigma\sqrt{T}} \tag{8}$$

$$d_2 = d_1 - \sigma\sqrt{T} \tag{9}$$

D. Heston model

Heston model has two separate processes, one for the stock price and one for the variance process[9]:

$$dS_t = rS_t dt + \sqrt{v_t} S_t dW_S(t) \tag{10}$$

$$dv_t = \kappa\left(\theta - v_t\right) dt + \sigma\sqrt{v_t} dW_v(t) \tag{11}$$

$$dW_s(t) dW_v(t) = \rho_{s,v} dt \tag{12}$$

where:

- r : risk-free interest rate
- v : variance ($v \geq 0$)
- κ : rate of reversion to the long-term variance
- θ : long-term variance ($\theta > 0$)
- σ : volatility of the variance ($\sigma \geq 0$)
- $dW_s(t), dW_v(t)$: two Wiener processes(correlated with a constant correlation ρ)

In Heston process, the stock process depends on a time-dependent variance process. The variance process is decided by the constant parameters: κ, θ, σ. If the reversion rate κ is high, the volatility will converge quickly to the long-term variance θ and vice versa. The correlation coefficient of the two Wiener processes are usually negative because of the leverage effect[2].

III. Numerical methods for SDEs

A. Monte Carlo method

Monte Carlo method is applicable to a wide-range of problems, and it works well in option pricing, especially for path-dependent options. This method is based on the *Central Limit Theorem* and the *Law of Large Numbers*. A Monte Carlo method approximating an option in a risk-neutral world involves the following step:

1) Partition the time interval $[0, T]$, the time step is $dt = \frac{T}{N}$, where N is number of time steps.
2) Simulate one path for the asset value S_i, $i = 1, ..., N$.
3) Repeat step 2 M times to get multiple asset paths, with M being the number of paths in Monte Carlo simulation.
4) Compute the M payoffs of option: $H_j = H(T, S_{i,j})$, $i = 1, ..., N$(steps), $j = 1, ..., M$(paths).
5) Discount mean payoff at risk free rate to get estimated of the option price:

$$V\left(t, S\right) \approx \mathrm{e}^{-r(T-t)} \frac{1}{M} \sum_{j=1}^{M} H_j$$

The standard error in Monte Carlo simulation is defined as:

$$\epsilon_M := \frac{\sigma_M}{\sqrt{M}} \tag{13}$$

where σ is the standard deviation of M estimated values.

B. Euler-Maruyama method

The Euler-Maruyama method is a generalisation of the Euler method for ordinary differential equations to stochastic differential equations and may be applied to an equation of the form

$$dX(t) = a(t, X(t))dt + b(t, X(t))dW(t) \tag{14}$$
$$\text{with } X(0) = X_0,\ 0 \leq t \leq T$$

where a and b are scalar functions and the initial condition $X(0)$ is a random variable. Given the functions a and b, the stochastic process $X(t)$ is a solution of Equation 14 if $X(t)$ solves the integral equation:

$$X(t) = X(0) + \int_0^t a(u, X(u))du + \int_0^t b(u, X(u))dW(u) \tag{15}$$

In practice, the above equation is not always explicitly solvable and hence we can't get an analytical solution $X(t)$ to a given *SDE*. But we can always get approximate

numerical solution of any given *SDE*. In particular, let $\hat{X}(t)$ denote a time-discretized approximation to $X(t)$. Suppose we discretize the interval $[0, T]$: let $\Delta t = \frac{T}{N}$ and $t_n = n\Delta t$, $n = 0, 1, 2, \cdots N$. The exact solution on the time grid would be:

$$X(t_{n+1}) = X(t_n) + \int_{t_n}^{t_{n+1}} a(u, X(u))du + \int_{t_n}^{t_{n+1}} b(u, X(u))dW(u) \quad (16)$$

Approximating the integrands by the left-hand rule we have :

$$\hat{X}(t_{i+1}) = \hat{X}(t_i) + a(t_i, \hat{X}(t_i))[t_{i+1} - t_i] + b(t_i, \hat{X}(t_i))[W(t_{i+1}) - W(t_i)]$$

$W(t_{i+1}) - W(t_i)$ and $\sqrt{t_{i+1} - t_i}Z$ have identical distribution, with $Z \sim \mathcal{N}(0, 1)$. The *Euler-Maruyama* approximation of Equation 16 is then given by:

$$\boxed{\hat{X}(t_{i+1}) = \hat{X}(t_i) + a(t_i, \hat{X}(t_i))\Delta t + b(t_i, \hat{X}(t_i))\sqrt{\Delta t}Z} \quad (17)$$

1) Euler scheme for the Black Scholes model: To apply the Euler Scheme to the Black Scholes, we start with the exact solution of Equation 4 in integral form as discussed in Equation 16. We then get:

$$S_{t+dt} = S_t + r\int_t^{t+dt} S_u du + \sigma\int_t^{t+dt} S_u dW(u) \quad (18)$$

Discretizing the integrals we get:

$$\int_t^{t+dt} S_u du \approx S_t dt$$
$$\int_t^{t+dt} S_u dW_u \approx S_t(W(t+dt) - W(t)) = \sqrt{dt}S_t Z$$

Putting back the integrand approximations in Equation 18, we get the Euler approximation to the Black Scholes model:

$$\boxed{S_{t+dt} = S_t + rS_t dt + \sigma\sqrt{dt}S_t Z} \quad (19)$$

2) Euler scheme for the Heston model: We can apply the Euler scheme to the Heston model in a similar way. We begin by the variance process in Equation 11 as:

$$v_{t+dt} = v_t + \int_t^{t+dt} \kappa(\theta - v_u)du + \int_t^{t+dt} \sigma\sqrt{v_u}dW_v(u) \quad (20)$$

Now, discretizing the above integrals as:

$$\int_t^{t+dt} \kappa(\theta - v_u)du \approx \kappa(\theta - v_t)dt$$
$$\int_t^{t+dt} \sigma\sqrt{v_u}dW_v(u) \approx \sigma\sqrt{v_t}(W_v(t+dt) - W_v(t)) = \sigma\sqrt{v_t dt}Z_v$$

Plugging the integrand approximations back in Equation 20 we have:

$$\boxed{v_{t+dt} = v_t + \kappa(\theta - v_t)dt + \sigma\sqrt{v_t dt}Z_v} \quad (21)$$

To avoid problems with negative values in $\sqrt{V_t}$, we may apply the *full truncation* or *reflection* scheme. We discuss about this in the section CIR process simulation.
For the S_t SDE we proceed similarly:

$$S_{t+dt} = S_t + r\int_t^{t+dt} S_u du + \int_t^{t+dt} \sqrt{v_u}S_u dW_s(u)$$

Discretizing we have:

$$\int_t^{t+dt} S_u du \approx S_t dt$$
$$\int_t^{t+dt} \sqrt{v_u}S_u dW_s(u) \approx \sqrt{v_t}S_t(W_s(t+dt) - W_s(t)) = \sqrt{v_t dt}S_t Z_s$$

Z_s is a standard normal variable with correlation ρ with Z_v. We have:

$$\boxed{S_{t+dt} = S_t + rS_t dt + \sqrt{v_t dt}S_t Z_s} \quad (22)$$

C. Milstein method

Inspection of the Euler scheme in Equation 17 from the perspective of Taylor expansion suggests a possible inconsistency: the approximation expands the drift to $\mathcal{O}(\Delta t)$ but the diffusion term only to $\mathcal{O}(\sqrt{\Delta t})$.This discrepancy suggests that to refine the Euler scheme we may want to focus on the diffusion term. *Glasserman*[4] and *Rouah*[10] describe the Milstein refinement for SDEs for which the coefficients do not depend on t directly. This reduces Equation 15 to:

$$X(t) = X(0) + \int_0^t a(X(u))du + \int_0^t b(X(u))dW(u)$$

As discussed earlier, the Euler scheme results from the approximations:

$$\int_{t_n}^{t_{n+1}} a(X(u))du \approx a(X(t_n))\Delta t$$

and

$$\int_{t_n}^{t_{n+1}} b(X(u))dW(u) \approx b(X(t_n))[W(t_{n+1}) - W(t_n)] \tag{23}$$

In both cases, we freeze the integrand at t_n over the interval $[t_n, t_{n+1}]$. To improve the approximation of the diffusion term, we need a better approximation of $b(X(u))$ over interval $[t_n, t_{n+1}]$. We therefore examine the evolution of $b(X(u))$. Applying Ito's lemma to $b(X(u))$ and noting that the derivatives w.r.t to t are 0, we get:

$$\begin{aligned} db(X(t)) = [b'(X(t))a(X(t)) + \frac{1}{2}b''(X(t))b^2(X(t))]dt \\ + b'(X(t))b(X(t))dW(t) \end{aligned} \tag{24}$$

where, b' and b'' are the first and second derivatives w.r.t $X(t)$. Now applying Euler approximation to Equation 24 with $t \leq u \leq t + \Delta t$:

$$\begin{aligned} b(X(u)) \approx b(X(t)) + \Bigg(b'(X(t))a(X(t)) \\ + \frac{1}{2}b''(X(t))b^2(X(t))\Bigg)[u-t] \\ + b'(X(t))b(X(t))[W(u) - W(t)] \end{aligned}$$

Now $W(u) - W(t) = \mathcal{O}(\sqrt{u-t})$ whereas the drift term in this approximation is $\mathcal{O}(u-t)$ and thus of higher order. Dropping this higher-order term yields:

$$\begin{aligned} b(X(u)) \approx b(X(t)) + b'(X(t))b(X(t))[W(u) - W(t)] \\ u \in [t, t + \Delta t]. \end{aligned}$$

With the above approximation, we can now refine Equation 23 as:

$$\begin{aligned} &\int_t^{t+\Delta t} b(X(u))dW(u) \approx \int_t^{t+\Delta t} \Bigg(b(X(t)) \\ &+ b'(X(t))b(X(t))[W(u) - W(t)]\Bigg)dW(u) \\ &= b(X(t))[W(t+\Delta t) - W(t)] \\ &+ b'(X(t))b(X(t))\left(\int_t^{t+\Delta t}[W(u) - W(t)]dW(u)\right) \end{aligned} \tag{25}$$

We simplify the last integral:

$$\begin{aligned} &\int_t^{t+\Delta t}[W(u) - W(t)]dW(u) \\ &\quad = \int_t^{t+\Delta t} W(u)dW(u) - W(t)\int_t^{t+\Delta t} dW(u) \\ &\quad = Y(t+\Delta t) - Y(t) \\ &\quad - W(t)[W(t+\Delta t) - W(t)] \end{aligned} \tag{26}$$

where

$$dY(t) = W(t)dW(t)$$

Using *Ito's* lemma, we can easily verify the solution of $Y(t)$ as $Y(t) = \frac{1}{2}(W(t))^2 - \frac{1}{2}t$. Making this substitution in Equation 26 and simplifying, we get:

$$\begin{aligned} \int_t^{t+\Delta t}[W(u) - W(t)]dW(u) = &\frac{1}{2}[W(t+h) - W(t)]^2 \\ &- \frac{1}{2}\Delta t \end{aligned}$$

Using this identity in Equation 25, we get:

$$\begin{aligned} \int_t^{t+\Delta t} b(X(u))dW(u) \approx b(X(t))[W(t+\Delta t) - W(t)] + \\ \frac{1}{2}b'(X(t))b(X(t))\left([W(t+\Delta t) - W(t)]^2 - \Delta t\right) \end{aligned}$$

Finally, we use this approximation to refine the one-step Euler approximation as:

$$\begin{aligned} X(t+\Delta t) \approx X(t) + a(X(t))\Delta t + b(X(t))[W(t+\Delta t) \\ - W(t)] + \frac{1}{2}b'(X(t))b(X(t))\Bigg([W(t+h) \\ - W(t)]^2 - \Delta t\Bigg) \end{aligned}$$

While performing MC simulations, we apply the above scheme recursively at $\Delta t, 2\Delta t, \ldots$ and replacing the increments of W with $\sqrt{\Delta t}Z$, to get:

$$\boxed{\begin{aligned} \hat{X}(t_{i+1}) = \hat{X}(t_i) + a(\hat{X}(t_i))\Delta t + b(\hat{X}(t_i))\sqrt{\Delta t}Z \\ + \frac{1}{2}b'(\hat{X}(t_i))b(\hat{X}(t_i))\Delta t(Z^2 - 1) \end{aligned}} \tag{27}$$

If we compare Equation 17 and Equation 27, we notice that the Milstein scheme adds a new term $\frac{1}{2}b'(\hat{X}(t_i))b(\hat{X}(t_i))\Delta t(Z^2-1)$. We will see in Section Convergence whether and in what sense this additional term is an improvement over the Euler scheme.

1) Milstein scheme for Black Scholes model: Applying the discretization in equation 27 to equation 4 we get the Milstein scheme for Black Scholes model, which is given by:

$$\boxed{\begin{aligned} S_{t+dt} &= S_t + rS_t dt + \sigma S_t \sqrt{dt} Z \\ &\quad + \frac{1}{2}\sigma^2 dt \left(Z^2 - 1\right) \end{aligned}} \tag{28}$$

2) Milstein scheme for Heston model: Similarly, if we apply Milstein discretization to the two stochastic processes in Heston model, we get:

$$\boxed{\begin{aligned} v_{t+dt} &= v_t + \kappa\left(\theta - v_t\right) dt + \sigma\sqrt{v_t dt} Z_v \\ &\quad + \frac{1}{4}\sigma^2 dt (Z_v^2 - 1) \end{aligned}} \tag{29}$$

$$\boxed{\begin{aligned} S_{t+dt} &= S_t + rS_t dt + \sqrt{v_t dt} S_t Z_s \\ &\quad + \frac{1}{2} S_t v_t dt \left(Z_s^2 - 1\right) \end{aligned}} \tag{30}$$

where $Z_s = \rho Z_1 + \sqrt{1-\rho^2} Z_2$, Z_1, Z_2 are two independent standard normal variables.

One thing worth noting is that in the Rouah paper[10], the stochastic process of the stock price was wrongly derived. Instead of Equation 29, the following expression was shown:

$$S_{t+dt} = S_t + rS_t dt + \sqrt{v_t dt} S_t Z_s + \frac{1}{4} S_t^2 dt (Z_s^2 - 1) \tag{31}$$

from which stock price paths cannot be successfully simulated. The effect of this error is further demonstrated in Section IV.

D. Convergence

Convergence formalizes what it means for one stochastic process to get closer to another as the discrete time steps Δt are reduced. The two most common type of convergences are *weak convergence* and *strong convergence*.

1) Weak convergence: Weak convergence criterion is based on the proximity of the corresponding distributions of a discretized process to a continuous process. The error term simply computes the error between the expected values of the two stochastic processes at a given point in time. For the weak convergence, we define the error term:

$$e_{\Delta t}^{\text{weak}} := |E(X(T)) - E(\hat{X}(T))| \tag{32}$$

2) Strong convergence: Strong convergence is based on the path-wise proximity of a discretized process to a continuous process. This captures the difference between the approximation and the exact solution at specific mesh points. Since, the difference is taken before computing the mean, strong convergence is more demanding than weak convergence.

For strong convergence we define the error term:

$$e_{\Delta t}^{\text{strong}} := E[|X(T) - \tilde{X}(T)|] \tag{33}$$

For both cases, a general discrete-time approximation converges weakly/strongly to the solution $X(t)$, if:

$$\lim_{\Delta t \to 0} e^i(\Delta t) = 0, \text{ where } i = \text{weak, strong.} \tag{34}$$

3) Order of convergence: In addition to knowing that errors shrink with respect to Δt, we are interested in how fast an approximation converges as we reduce Δt. An approximation is said to converge weakly/strongly with order γ, if there exists a constant C, such that:

$$e_{\Delta t}^i \leq C \Delta t^\gamma, \text{ where } i = \text{weak, strong.} \tag{35}$$

A larger value of γ implies faster convergence to zero of the discretization error. The same scheme will often have a smaller strong order of convergence than its weak order of convergence. *Kloeden & Platen*[7] showed that the Euler scheme has a strong order of $\frac{1}{2}$ and weak order of 1 (under some smoothness conditions [7] of coefficients a and b). *Kloeden & Platen*[7] and *Talay*[11] provide conditions under which Milstein's scheme have a strong order of 1. However, the weak order of convergence for the Milstein scheme is 1. This may seem counter intuitive considering that including additional terms as in Equation 27 does not result in greater accuracy. This is because option payoffs are typically non-differentiable, while most of these conditions require significant smoothness assumptions. So, it is essential to test the methods numerically to find the order of convergence of any discretization scheme, specifically higher-order schemes.

E. CIR process simulation

There is no close-form price for path-dependent exotic options under Heston's model. However, we still need a baseline to measure the performance of our numerical simulations. We use the *Almost exact scheme* which employs sampling from the non-central chi-squared distribution of the CIR process. The sampled CIR paths are then used to generate baseline prices for the exotic options, using a very fine time grid and large Monte Carlo paths. This removes significant bias and errors

from brute force MC simulations, as we are sampling from the exact distribution of CIR process.

The variance process in Heston stochastic volatility model is a Cox-Ingersoll-Ross(CIR) process:

$$dv(t) = \kappa(\theta - v(t))dt + \sigma\sqrt{v(t)}dW(t) \tag{36}$$

For some initial variance $v(t_0) = v_0$, the variance $v(t)$ is distributed as $\bar{c}$ times a non-central chi-squared random variable, $\chi^2(\bar{d}, \bar{\lambda}(t))$, where $\bar{d}$ is the degrees of freedom parameter and $\bar{\lambda}(t)$ is the non-centrality parameter.

$$v(t) \sim \bar{c}(t)\chi^2(\bar{d}, \bar{\lambda}(t)),\ t > 0$$

with

$$\bar{c}(t) = \frac{1}{4\kappa}\sigma^2(1 - e^{-\kappa t}),\ \bar{d} = \frac{4\kappa\theta}{\sigma^2}$$
$$\bar{\lambda}(t) = \frac{4\kappa v_0 e^{-\kappa t}}{\sigma^2(1 - e^{-\kappa t})}$$

The above formulation forms the basis for an exact simulation scheme for the path realizations of the CIR process. It is also important to note that the square-root process for variance precludes negative values for $v(t)$. The *Feller Condition*, $2\kappa\theta \geq \sigma^2$, guarantees that $v(t)$ stays positive; otherwise, the variance process may reach zero.[9]. The square-root in the CIR process prevents negative $v(t)$, but the discretization schemes can not guarantee the non-negative realizations. Thus, we will introduce two schemes dealing with the possible negative path of $v(t)$.

1) Truncated scheme: The first scheme is truncating all the negative realizations.

$$\begin{aligned}\hat{v}_{i+1} &= v_i + \kappa(\theta - v_i)\Delta t + \sigma\sqrt{v_i \Delta t}Z \\ v_{i+1} &= max(\hat{v}_{i+1}, 0)\end{aligned} \tag{37}$$

2) Reflecting scheme: Another possible modification for negativity is using the reflecting principle which forces the CIR process to move upwards.

$$\begin{aligned}\hat{v}_{i+1} &= v_i + \kappa(\theta - v_i)\Delta t + \sigma\sqrt{v_i \Delta t}Z \\ v_{i+1} &= |\hat{v}_{i+1}|\end{aligned} \tag{38}$$

The distribution of CIR process paths has the following expected value and variance:

$$\begin{aligned}\mathbb{E}[v_t|v_0] &= v_0 e^{-\kappa t} + \theta(1 - e^{-\kappa t}) \\ Var[v_t|v_0] &= v_0\frac{\sigma^2}{\kappa}(e^{-\kappa t} - e^{-2\kappa t}) + \frac{\theta\sigma^2}{2\kappa}(1 - e^{-\kappa t})^2\end{aligned} \tag{39}$$

F. Almost Exact Solution of Heston[9]

Let $x(t) := logS(t)$, the Heston model described by equation 10 and 11 becomes:

$$dx(t) = (r - \frac{1}{2}v(t))dt + \sqrt{v(t)}dW_x(t) \tag{40}$$
$$dv(t) = \kappa(\theta - v(t))dt + \sigma\sqrt{v(t)}dW_v(t) \tag{41}$$

After integrating both processes above in a certain time interval $[t_i, t_{i+1}]$, we obtain the following discretization:

$$\begin{aligned}x_{i+1} = x_i &+ \int_{t_i}^{t_{i+1}} \left(r - \frac{1}{2}v(t)\right)dt \\ &+ \rho_{x,v}\int_{t_i}^{t_{i+1}} \sqrt{v(t)}d\widetilde{W}_v(t) \\ &+ \sqrt{1 - \rho_{x,v}^2}\int_{t_i}^{t_{i+1}} \sqrt{v(t)}d\widetilde{W}_x(t)\end{aligned} \tag{42}$$

$$\begin{aligned}v_{i+1} = v_i &+ \kappa\int_{t_i}^{t_{i+1}} (\theta - v(t))dt \\ &+ \sigma\int_{t_i}^{t_{i+1}} \sqrt{v(t)}d\widetilde{W}_v(t)\end{aligned} \tag{43}$$

The two integrals with $\widetilde{W}_v(t)$ above are the same. After re-arranging equation 43 we have:

$$\begin{aligned}\int_{t_i}^{t_{i+1}} \sqrt{v(t)}d\widetilde{W}_v(t) = \frac{1}{\sigma}[&v_{i+1} - v_i \\ &- \kappa\int_{t_i}^{t_{i+1}} (\theta - v(t))dt]\end{aligned} \tag{44}$$

where v_{i+1} can be simulated by CIR process as previously discussed.

The discretization for x_{i+1} in equation 42 becomes:

$$\begin{aligned}x_{i+1} = x_i &+ \int_{t_i}^{t_{i+1}} \left(r - \frac{1}{2}v(t)\right)dt \\ &+ \frac{\rho_{x,v}}{\sigma}\left(v_{i+1} - v_i - \kappa\int_{t_i}^{t_{i+1}} (\theta - v(t))dt\right) \\ &+ \sqrt{1 - \rho_{x,v}^2}\int_{t_i}^{t_{i+1}} \sqrt{v(t)}d\widetilde{W}_x(t)\end{aligned} \tag{45}$$

We approximate all the integrals in equation 45 by left integration as in Euler discretization scheme:

$$\begin{aligned}x_{i+1} \approx x_i &+ \left(r - \frac{1}{2}v_i\right)\Delta t \\ &+ \frac{\rho_{x,v}}{\sigma}\left(v_{i+1} - v_i - \kappa\left(\theta - v_i\right)\Delta t\right) \\ &+ \sqrt{1 - \rho_{x,v}^2}\sqrt{v_i}\left(\widetilde{W}_x\left(t_{i+1}\right) - \widetilde{W}_x\left(t_i\right)\right)\end{aligned} \tag{46}$$

After collection of all terms and using the property of normal distribution:

$$\widetilde{W}_x\left(t_{i+1}\right) - \widetilde{W}_x\left(t_i\right) \overset{d}{=} \sqrt{\Delta t}Z_x,\ \text{with}\ Z_x \sim N(0, 1)$$

The almost exact simulation of Heston model is given by:

$$x_{i+1} \approx x_i + k_0 + k_1 v_i + k_2 v_{i+1} + \sqrt{k_3} v_i Z_x \quad (47)$$

$$v_{i+1} = \bar{c}\left(t_{i+1}, t_i\right) \chi^2\left(\delta, \bar{\kappa}\left(t_{i+1}, t_i\right)\right) \quad (48)$$

with:

$$\bar{c}\left(t_{i+1}, t_i\right) = \frac{\sigma^2}{4\kappa}\left(1 - \mathrm{e}^{-\kappa(t_{i+1} - t_i)}\right), \quad \delta = \frac{4\kappa\theta}{\sigma^2}$$

$$\bar{\kappa}\left(t_{i+1}, t_i\right) = \frac{4\kappa \mathrm{e}^{-\kappa\Delta t}}{\sigma^2\left(1 - \mathrm{e}^{-\kappa\Delta t}\right)} v_i$$

$$k_0 = \left(r - \frac{\rho_{x,v}}{\sigma}\kappa\theta\right)\Delta t,$$

$$k_1 = \left(\frac{\rho_{x,v}\kappa}{\sigma} - \frac{1}{2}\right)\Delta t - \frac{\rho_{x,v}}{\sigma}$$

$$k_2 = \frac{\rho_{x,v}}{\sigma}, \quad k_3 = \left(1 - \rho_{x,v}^2\right)\Delta t$$

IV. Methods and Results

We first analysed how the Euler and Milstein discretization compare to the analytical solutions and tried to verify their order of convergences. Figure 1 shows a sample solution path from *Geometric Brownian Motion* plotted against the Euler and Milstein approximations. We observe that at smaller time steps (finer grid), both the schemes approximate the analytical solution quite well. Increasing the time steps (coarser grid), however, deteriorated the Euler approximations as shown in the bottom panel of Figure 1. In Figure 2, we observe that the experimental strong and weak convergence orders of Euler and Milstein schemes are quite close to the theoretical values. However, we also found that to observe the theoretical order of convergences, the schemes required specific smoothness conditions on the drift and diffusion coefficients, which we discussed in section Convergence.

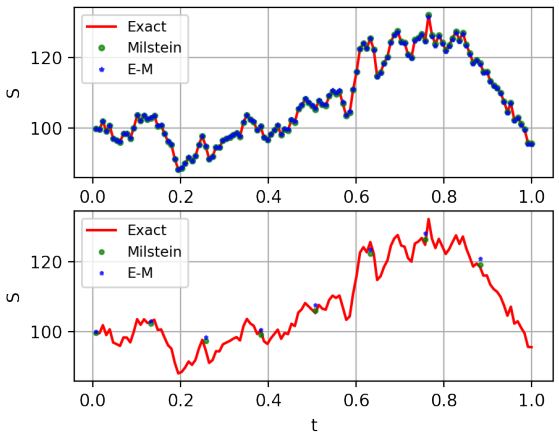

Fig. 1: Black-Scholes model simulation of a stock price path using EM and Milstein schemes. $S_0 = 100$, $T = 1$, $r = 0.01$ and $\sigma = 0.25$. EM scheme with **(Top)** finer ($N = 128$) and **(Bottom)** coarser ($N = 8$) grids in time domain. Comparison of EM and Milstein schemes to analytical solution.

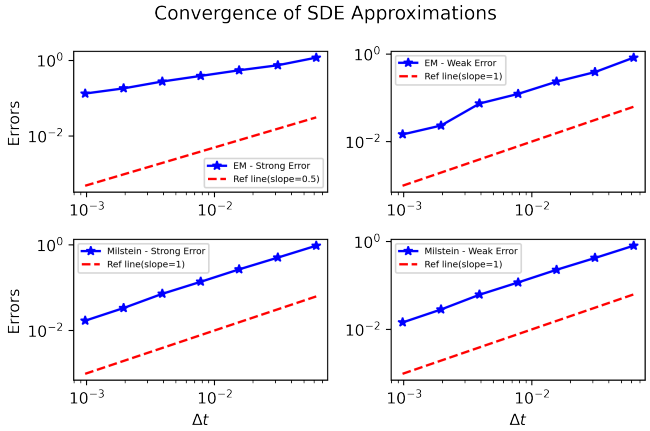

Fig. 2: Convergence of EM and Milstein schemes with 10000 Monte-Carlo paths. $S_0 = 1$, $T = 1$, $r = 2$ and $\sigma = 1$. **(Top left)** EM strong error. **(Top right)** EM weak error. **(Bottom left)** Milstein strong error. **(Bottom right)** Milstein weak error.

A. Black-Scholes model

The options we considered under Black-Scholes model were a European put and Down-and-out put option. The analytical solutions for both these options were used as baseline values and taken from *Hull*[6]. We performed the Euler and Milstein discretizations using MC simulations with $M = 200,000$ paths averaged over 10 iterations to compute the option prices. As can be seen in Figure 3, choosing $200,000$ MC paths produced around €0.02 standard error for European put option and €0.01 standard error for the Down-and-out put option. We run the Euler and Milstein schemes with $N = [252, 52, 12, 4]$ time steps corresponding to daily, weekly, monthly and quarterly time steps. Then the results of sequentially varying the model parameters are visualised as in Figure 4, 5 and 6. The plots show the absolute errors w.r.t to the baseline values and the correction term Milstein scheme introduces on the secondary $y-$axis. In addition, we also show the corresponding standard errors in the option prices at the grid points with a *black* candlestick for Heston and *red* candlestick for Euler approximations. We don't show results from our full parameter search simulations as this would make the

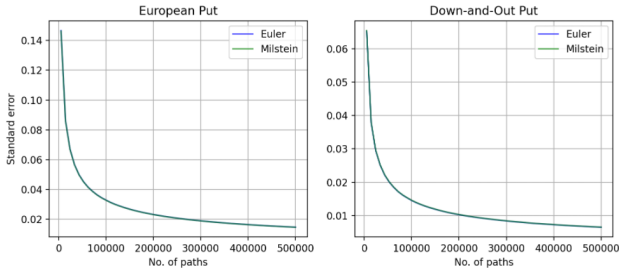

Fig. 3: Standard errors for option prices $S_0 = 100$, $T = 1$, $r = 0.15\%$, $N = 52$, $K = 100$, $H = 80$ and $\sigma = 20\%$.**(Left)** European Put. **(Right)** Down-and-out Put.

Figures less clear.

Figure 4, shows the effect of varying interest rates. We observe that at very low interest rates, Milstein errors are lower than Euler errors for European options. However, for $r > 1\%$ Milstein performs worse than the Euler scheme at coarser time steps. For Barrier options, we observe that the Milstein errors are consistently higher than Euler at coarser time steps.

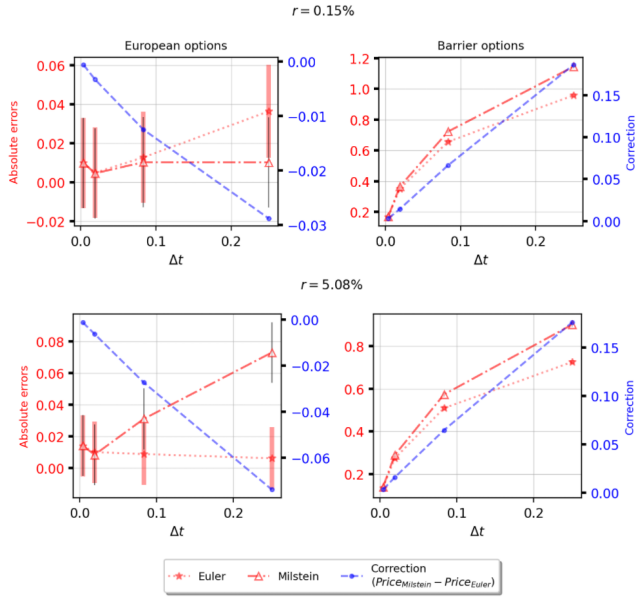

Fig. 4: Varying interest rates. *Fixed parameters:* $S_0 = 100$, $T = 1$ *yr*, $K = 100$, $H = 80$ *and* $\sigma = 20\%$

In Figure 5 we observe that for European options, at very low volatilities (10%) Milstein scheme does not outperform Euler. However, increasing the volatility significantly improves the Milstein approximations as compared to Euler. For Barrier options, the Euler scheme performs better.

Figure 6 shows the effect of varying barrier prices on down-and-out put prices. We observe that for $H < K$, Euler scheme produces less discretization errors than

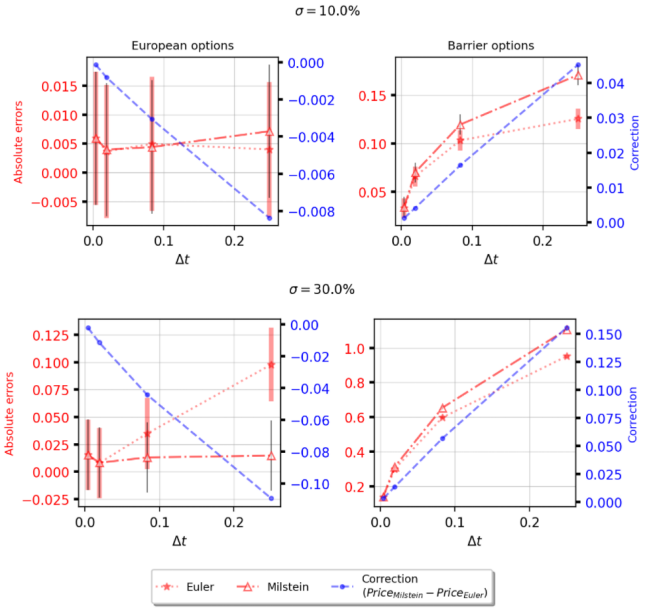

Fig. 5: Varying volatility. *Fixed parameters:* $S_0 = 100$, $T = 1$ *yr*, $r = 1\%$, $K = 100$, $H = 80$

Milstein. Increasing the barrier H and taking it closer to the strike price, results in almost same errors with both the schemes.

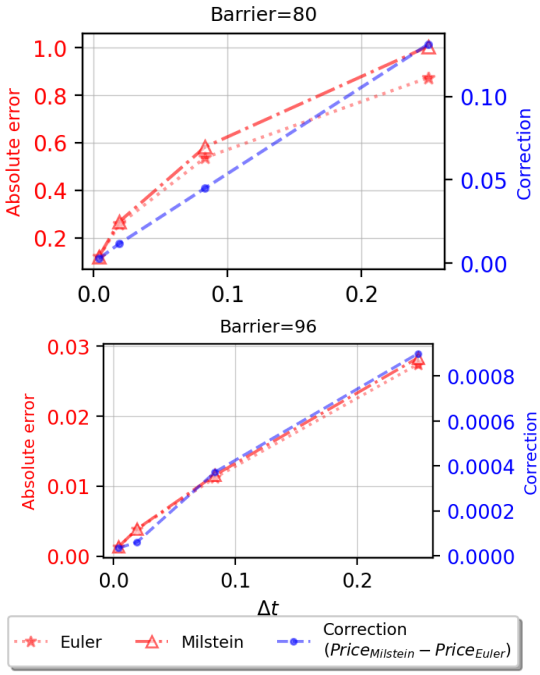

Fig. 6: Varying barrier. *Fixed parameters:* $S_0 = 100$, $T = 1$ *yr*, $r = 1\%$, $K = 100$, $\sigma = 35\%$

B. Heston model

For the Heston model, we considered a European and a Down-and-out call option. The semi-exact solutions

for the European option were computed using Fourier cosine series expansion (COS) method , while for the down-and-out call option we used the *Almost Exact Scheme*[9] with $120,000$ MC paths and $N = 2^{10}$ time steps as the baseline value. The time steps were taken as in the Black-Scholes model, ranging from daily to quarterly steps. An initial stock price of $S_0 =$€100 and strike price $K =$€100 was considered. The correlation between stock price and volatility is normally negative, since the volatility of the market tends to increase when the stock price goes down. Therefore, a correlation of $\rho = -0.7$ was chosen. The values of other parameters v_0, θ, κ and σ were taken from Crisostomo[3], which generally reflect the dynamics of the real market.

Figure 7 shows, one path of simulated stock price using both the EM and Milstein schemes, while the wrong expression of Equation 31 was used for Milstein discretization. A corrected version was then applied and the resulted paths of stock price and volatility can be found in Figure 8.

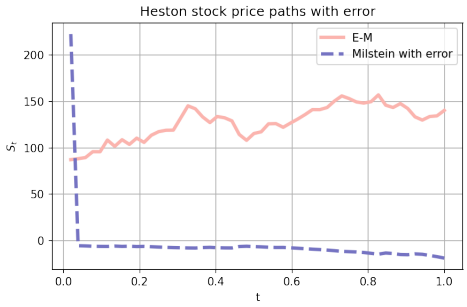

Fig. 7: Heston model simulation of a stock price path using the wrong expression of Milstein scheme. $N = 52$, $S_0 = 100$, $v_0 = 0.2$, $r = 0.01$, $\kappa = 6$, $\theta = 0.2$, $\sigma = 0.2$ and $\rho = -0.7$

To validate that the volatility paths are legit, we used the properties of the CIR process. Monte-Carlo simulation was run for 10000 paths for both EM and Milstein schemes, and the expected value and variance of the paths over time were computed. These values were plotted on Figure 9 together with the values calculated from Equation 39.

Figure 11 shows the effect of changing interest rates on the option pricing errors. We observe that the Milstein errors are consistently lower than the Euler errors for both European and Barrier options.

In Figure 12 we observe that for lower values of the volatility of volatility parameter, Euler and Milstein errors were quite low and almost equal to each other for both European and Barrier options. However, increasing the parameter significantly increases the discretization

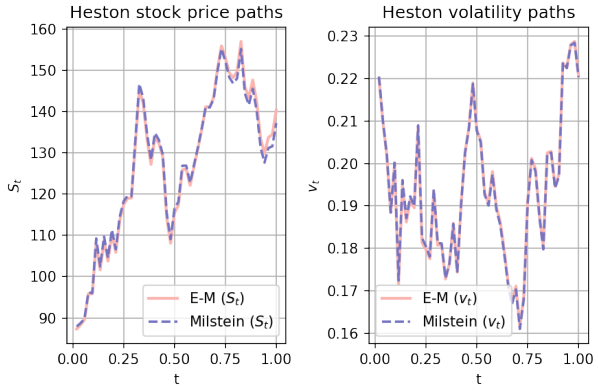

Fig. 8: Heston model simulation with EM and Milstein schemes. $N = 52$, $S_0 = 100$, $v_0 = 0.2$, $r = 0.01$, $\kappa = 6$, $\theta = 0.2$, $\sigma = 0.2$ and $\rho = -0.7$ **(Left)** Stock price. **(Right)** Volatility.

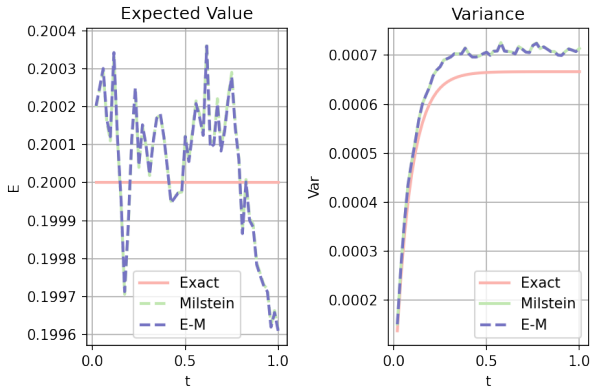

Fig. 9: The expect value and variance of 10000 simulated paths of volatility. $N = 52$, $\kappa = 6$, $\theta = 0.2$ and $\sigma = 0.2$. **(Left)** Expected value. **(Right)** Variance.

errors, with Milstein performing better than Euler. For barrier options, we observe the same trend.

Figure 13 shows that for lower values of reversion rates, κ, Milstein simulations are more accurate than Euler. However, errors from both the schemes approach equality with increasing values of κ. The down-and-out call option also exhibit this pattern.

Comparing the discretization errors in European call option prices in Figure 14, we observe that both the schemes exhibit an error reduction by a factor of 10 when the long-term variance θ increases from 0.1 to 0.54. The barrier options don't show any such trend with the errors. However, increase in θ brings the errors from Euler and Milstein schemes closer for both the option types.

From Figure 15 we observe that, increasing the initial variance v_0, increases the errors in both the schemes, with Milstein performing much better at lower values of

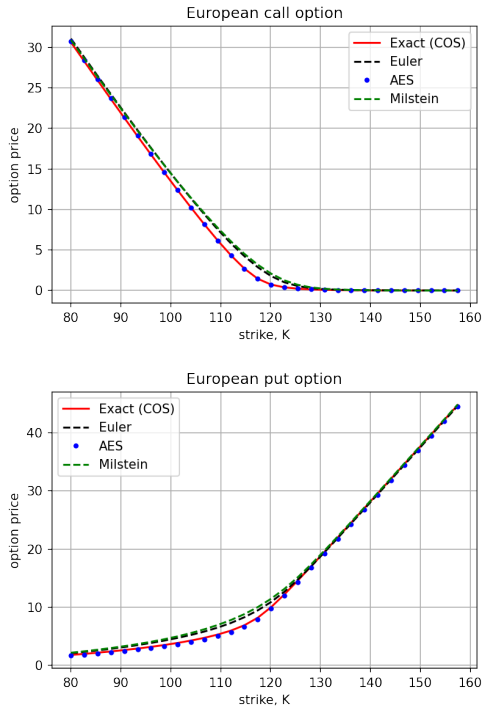

Fig. 10: Option pricing using different numerical schemes. $M = 10000$, $S_0 = 105$, $v_0 = 0.05$, $\theta = 0.05$, $T = 1$, $\kappa = 0.5$, $r = 0.05$, $\sigma = 1$ and $\rho = -0.9$. **(Top)** European call option. **(Bottom)** European put option.

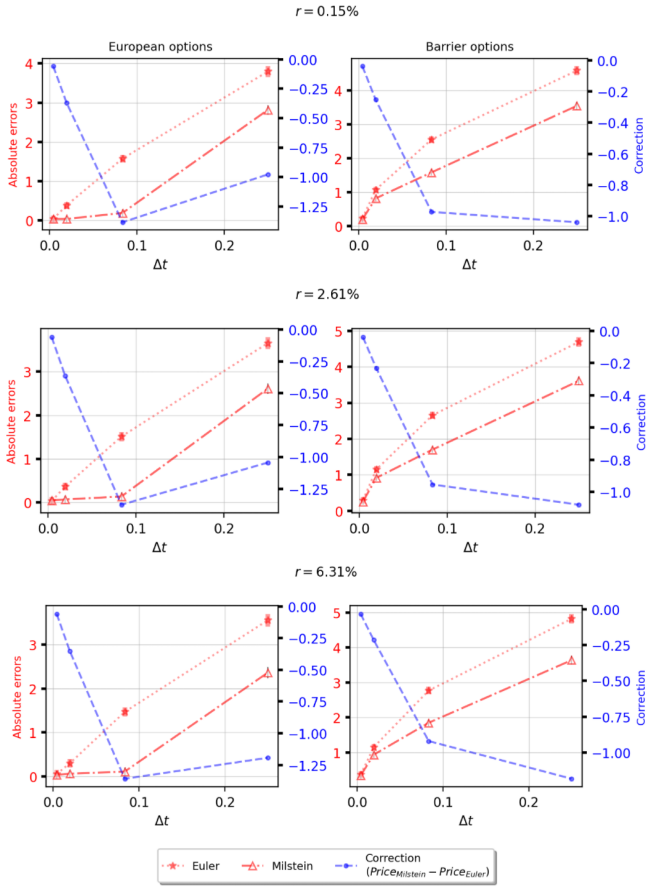

Fig. 11: Varying interest rates. *Fixed parameters:* $S_0 = 100$, $K = 100$, $H = 80$, $T = 1$ *yr*, $\sigma = 1.4$, $\rho = -0.7$, $\kappa = 6$, $v_0 = 0.2$, $\theta = 0.2$

v_0. Very high initial variances result in almost same error from both the schemes.

Varying the correlation ρ, resulted in marginal variations in errors from both the schemes. The Milstein errors are consistently lower than Euler's as shown in Figure 16.

In the specific case of Barrier options, barrier prices lower than the strike resulted in lower Milstein errors than Euler, as shown in Figure 17. However, taking the barrier close to the strike price, leads to roughly the same error with Euler and Milstein scheme.

V. Discussion

A. Black-Scholes model

It is clear from the expression of Milstein discretization for Black Scholes model, that the correction term $\frac{1}{2}\sigma^2 dt(Z^2 - 1)$ contributes to the added accuracy at higher volatilities. This explains why we see lower Milstein errors at higher volatilities in Figure 5. The higher Milstein errors with increasing interest rates in Figure 4 can be attributed to the fact that the above correction term also contains a random variable, Z. Thus at lower volatilities the stochastic effects are more likely to overwhelm the correction introduced by the lower volatility term, which makes the Milstein scheme less accurate. For barrier option pricings, we observed that taking the barrier closer to the strike level lead to both the schemes performing equally well. We hypothesize the reason to be the cut-off nature of barrier options which gives the option zero value when the barrier levels are breached. Therefore at significantly lower barrier levels, the asset is less likely to reach the barrier and correction term is more likely to introduce stochastic errors.

B. Heston model

It is obvious in Figure 7 that the wrong derivation of Rouah[10] would yield simulated stock paths that don't make sense. While the price of a normal stock oscillates around the initial price and has a general trend of increasing according to the interest rate, the path generated from Equation 31 first shoots up way above S_0 then goes below zero. This is due to the correction term $\frac{1}{4}S_t^2 dt(Z_s^2 - 1)$ in the wrong expression instead of the right one $\frac{1}{2}S_t v_t dt(Z_s^2 - 1)$. By squaring the stock price S_t term and neglecting the volatility v_t, the

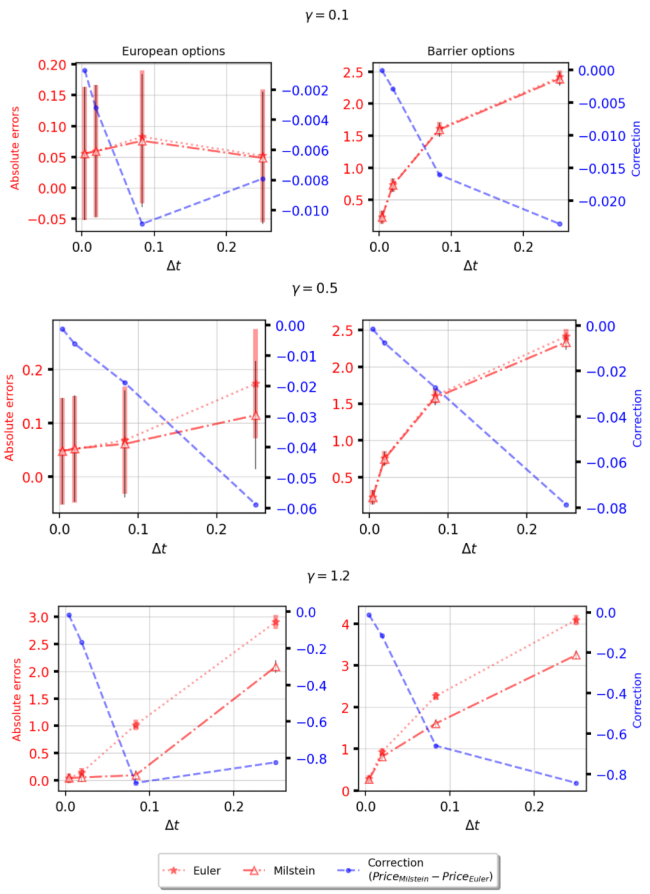

Fig. 12: Varying volatility of volatility. *Fixed parameters:* $S_0 = 100$, $K = 100$, $H = 80$, $T = 1$ *yr*, $r = 1\%$, $\rho = -0.7$, $\kappa = 6$, $v_0 = 0.2$, $\theta = 0.2$

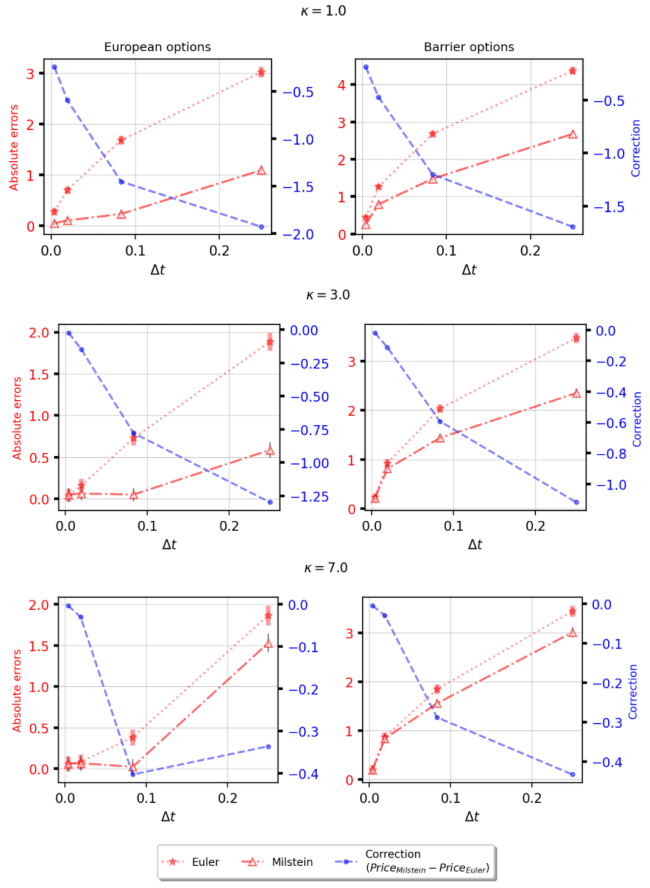

Fig. 13: Varying rate of reversion. *Fixed parameters:* $S_0 = 100$, $K = 100$, $H = 80$, $T = 1$ *yr*, $r = 1\%$, $\rho = -0.7$, $\sigma = 1$, $v_0 = 0.2$, $\theta = 0.2$

contribution of S_t was exaggerated and v_t not accounted for. If the wrong expression was used for option pricing, the resulted price would not make sense, since a stock price below zero does not have meanings in reality and it would yield negative option prices in the case of European call option.

Both of the corrected version of stock price and volatility simulation paths can be found in Figure 8. With a weekly realization ($N = 52$), the difference between EM and Milstein schemes in volatility paths is negligible. However, since the Heston model consists of two SDEs, small deviations in volatility can propagate into the simulation of stock price paths. We can see from the left panel of Figure 8 that slight differences can be observed as the stock price progress in time. The errors cannot be quantified at this stage due to lack of analytical solution, but will be further analyzed when pricing options.

Although the validity of the stock prices paths simulated cannot be verified yet, Figure 9 has shown that the volatility paths are correct ones. It can be seen that in the left panel, the expected value of 10000 paths fluctuates around the exact value in a very small range. The exact value was intentionally held at a constant level by setting both v_0 and θ to 0.2 for better demonstration. For the comparison of variance value in the right panel, the discretization schemes have slightly higher variances than the exact one calculated from CIR property. This is due to the coarse time steps ($N = 52$) and insufficient Monte-Carlo paths (10000). The variance can be reduced by using smaller time steps or more simulation paths, but it is tolerable in this case. Again, in Figure 9, the performance of EM and Milstein schemes are quite similar.

The results in Figure 11 to 17 were produced from simulations around calibrated parameters. So the trends we observed are expected to be quite stable and explainable. For all the choices of parameters presented, the Milstein scheme outperformed the EM scheme, which confirms that Milstein is a better choice when pricing options under realistic circumstances (i.e. weekly to quarterly evaluation). The general case is that the

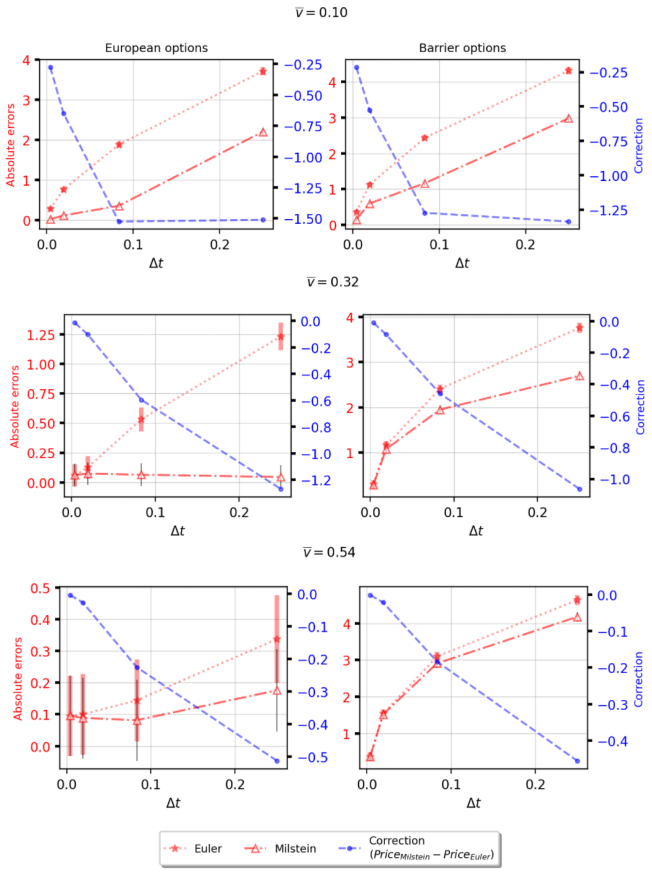

Fig. 14: Varying long term variance. *Fixed parameters:* $S_0 = 100$, $K = 100$, $H = 80$, $T = 1$ *yr*, $r = 1\%$, $\rho = -0.7$, $\sigma = 1$, $v_0 = 0.2$, $\kappa = 2$

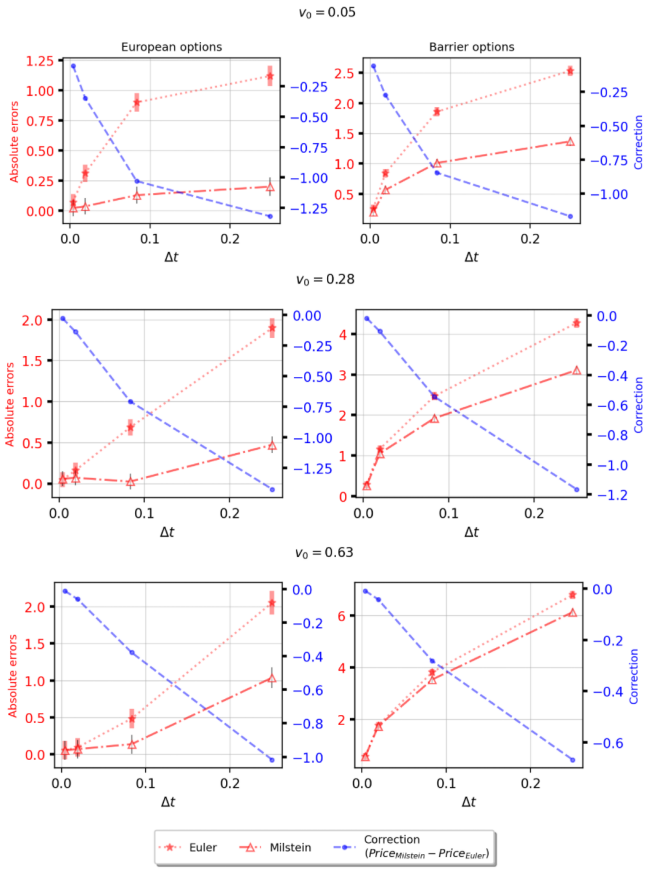

Fig. 15: Varying initial variance. *Fixed parameters:* $S_0 = 100$, $K = 100$, $H = 80$, $T = 1$ *yr*, $r = 1\%$, $\rho = -0.7$, $\sigma = 1$, $\theta = 0.25$, $\kappa = 2$

standard error of Monte-Carlo simulation is higher with the EM scheme than with the Milstein scheme. This is because the dt element in the correction term corrects for the error that occurs when the time grid gets coarser. From all these figures, we can say that the resulted option prices converge faster with barrier options than with European options, which also applies to the standard errors. By combining this observation with the results in Figure 2, we can argue that the Milstein scheme performs better on path-dependent options because it exhibits a faster strong convergence.

VI. Conclusion

In this paper, we have studied two widely used numerical schemes in option pricing: the Euler-Maruyama scheme and the Milstein scheme. We found that while both schemes have the same order of weak convergence, the Milstein scheme exhibits better strong convergence, implying that it can be a better choice when one needs to price a path-dependent option. The performance of both schemes were explored on path-independent European options and path-dependent barrier options by employing Monte-Carlo simulation of stock price paths. We can conclude that in real-life situations, the Milstein scheme is a more efficient and accurate way to price options, because it takes into account the coarser discretization of time domain, allowing less frequent evaluation and less expensive computation.

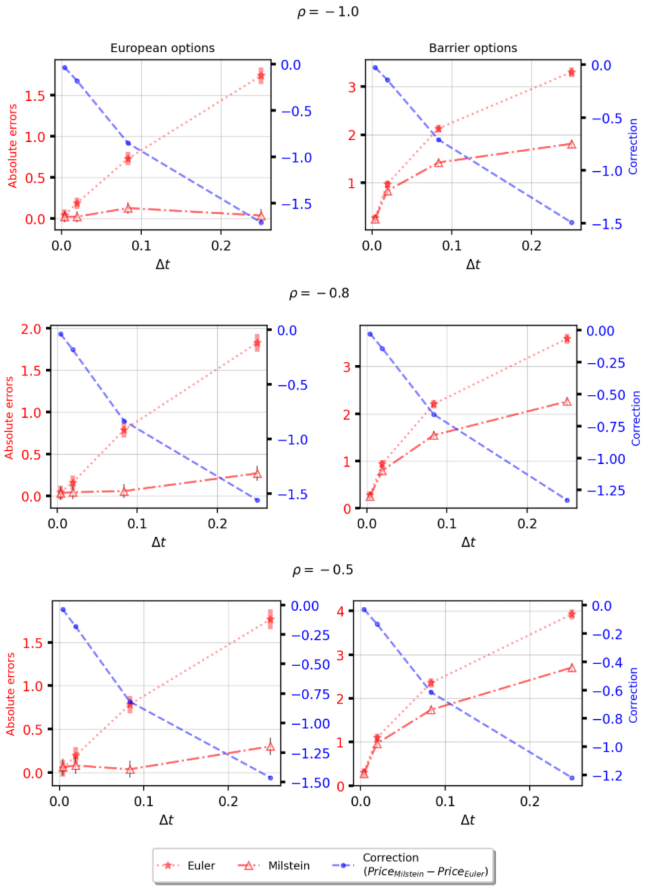

Fig. 16: Varying correlation. *Fixed parameters:* $S_0 = 100$, $K = 100$, $H = 80$, $T = 1$ *yr*, $\sigma = 1$, $r = 1\%$, $\kappa = 1$, $v_0 = 0.2$, $\theta = 0.25$

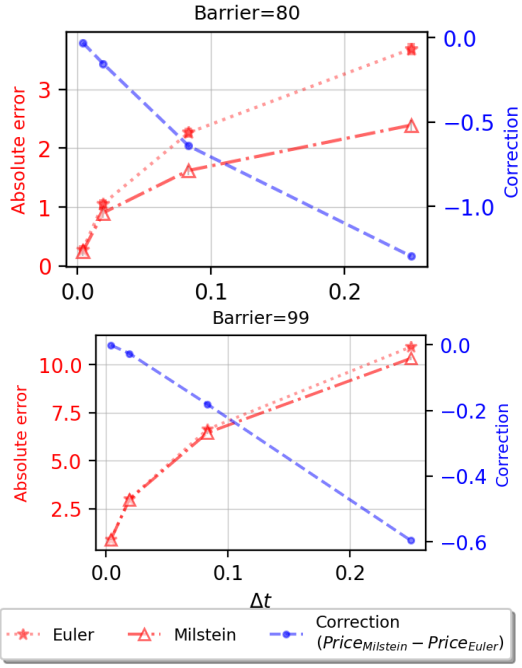

Fig. 17: Varying barrier. *Fixed parameters:* $S_0 = 100$, $K = 100$, $T = 1$ *yr*, $\sigma = 1$, $r = 1\%$, $\kappa = 1$, $\rho = -0.7$, $v_0 = 0.2$, $\theta = 0.25$

REFERENCES

[1] Abukar M Ali. "Exotic Options: Pricing Path-Dependent single Barrier Option contracts". In: ().

[2] Jean-Philippe Bouchaud, Andrew Matacz, and Marc Potters. "Leverage effect in financial markets: The retarded volatility model". In: *Physical review letters* 87.22 (2001), p. 228701.

[3] R. Crisostomo. "An Analysis of the Heston Stochastic Volatility Model: Implementation and Calibration using Matlab". In: *CNMV Working Paper* 58 (2014), pp. 1–46.

[4] Paul Glasserman. *Monte Carlo methods in financial engineering*. Vol. 53. Springer Science & Business Media, 2013.

[5] S. L. Heston. "A Closed-Form Solution for Options with Stochastic Volatility with Application to Bond and Currency Options". In: *The Review of Financial Studies* (1993).

[6] John C Hull. *Options futures and other derivatives*. Pearson Education India, 2003.

[7] Peter E Kloeden and Eckhard Platen. "Stochastic differential equations". In: *Numerical Solution of Stochastic Differential Equations*. Springer, 1992, pp. 103–160.

[8] G. N. Milstein. "Approximate integration of stochastic differential equations". In: *Theory of Probability & Its Applications* 19.3 (1974), pp. 583–588.

[9] Cornelis W Oosterlee and Lech A Grzelak. *Mathematical Modeling and Computation in Finance: With Exercises and Python and Matlab Computer Codes*. World Scientific, 2019.

[10] Fabrice Douglas Rouah. "Euler and milstein discretization". In: *Documento de trabajo, Sapient Global Markets, Estados Unidos. Recuperado de www. frouah. com* (2011).

[11] Denis Talay. "How to discretize stochastic differential equations". In: *Nonlinear filtering and stochastic control*. Springer, 1982, pp. 276–292.